

Collective motions in globally coupled tent maps with stochastic updating

Satoru Morita*

Department of Systems Engineering, Shizuoka University, 3-5-1 Johoku, Hamamatsu 432-8561, Japan

Tsuyoshi Chawanya

Department of Mathematics, Graduate School of Science, Osaka University, Toyonaka 560-0043, Japan

(Dated: November 21, 2018)

We study a generalization of globally coupled maps, where the elements are updated with probability p . When p is below a threshold p_c , the collective motion vanishes and the system is the stationary state in the large size limit. We present the linear stability analysis.

PACS numbers: 05.45.Jn, 05.70.Ln, 82.40.Bj

I. INTRODUCTION

The globally coupled maps (GCM) are introduced as a simple model capturing the essential features of nonlinear dynamical systems with many degrees of freedom [1]. One of the most interesting phenomena seen in such systems is the emergence of the collective motion [2, 3, 4]. The collective motion is characterized by a time dependence of the macroscopic variable in the large size limit [5, 6, 7, 8, 9, 10, 11, 12, 13, 14, 15, 16]. In this paper, we consider a variation of GCM to include asynchronous updating.

The general form of GCM is written in the following way

$$x_{t+1}(i) = f(x_t(i)) + \frac{K}{N} \sum_{i'=1}^N g(x_t(i')), \quad (1)$$

where t represents discrete time steps, i specifies each element, K gives the coupling strength, and N is the system size. All elements are updated synchronously in the deterministic way through the mean field

$$h_t \equiv \frac{1}{N} \sum_{i=1}^N g(x_t(i)). \quad (2)$$

Since the collective motions have been studied analytically in globally coupled tent maps [5, 6, 7, 8, 9, 10, 11, 12, 13], we specifically consider tent maps as follows:

$$\begin{aligned} f(x) &\equiv a \left(\frac{1}{2} - |x| \right), \\ g(x) &\equiv f(x) - \bar{f}. \end{aligned} \quad (3)$$

Here \bar{f} is a constant determined from the average of $f(x)$ over the the natural invariant measure of the map $x \mapsto f(x)$, i.e.,

$$\bar{f} = \int f(x) \rho_*(x) dx, \quad (4)$$

where $\rho_*(x)$ represents the the natural invariant density. By the above choice of $g(x)$, $h_t = 0$ is a stationary solution for the large size limit ($N \rightarrow \infty$) of (1), and the corresponding stationary distribution is proportional to $\rho_*(x)$. Equation (3) looks a little different from well-known form of GCM system

$$x_{t+1}(i) = (1 - \epsilon) f(x_t(i)) + \frac{\epsilon}{N} \sum_i f(x_t(i)), \quad (5)$$

which is obtained as a mean-field approximation for the coupled map lattice with diffusion coupling. In the case of the tent map system, however, the diffusion form (5) is scaled into (1) [12].

The collective motions in GCM (1) with (3) are classified into two types according to the gradient a of the tent map. First, in the case of $a < 1$, the synchronized chaos is stable. In this case, the map $x \mapsto f(x)$ has the stable fixed point

$$x_* = \frac{a}{2a+2}. \quad (6)$$

Thus, $\rho_*(x) = \delta(x - x_*)$, i.e., $g(x) = f(x) - f(x_*)$. Since the gradient of $f(x)$ is smaller than 1, the difference between any pair of elements diminishes. Thus all the elements behave identically after some initial transient. Here we concentrate on the long-term behavior and assume the system is one-cluster state. Then temporal evolution for x_t and h_t is obtained as follows

$$\begin{aligned} x_{t+1} &= \left[\frac{1}{2} + \frac{aK}{2+2a} - (1+K)|x_t| \right] \\ h_{t+1} &= a[x_* - |x_* + (1+K)h_t|]. \end{aligned} \quad (7)$$

When K is so large that $a(1+K) > 1$, the fixed point $h_t = 0$ is unstable. Then, the motion of the mean field is one-dimensional chaos, which obeys (7).

Second, in the case of $a > 1$, all elements are fully desynchronized and behave as if they are mutually independent. Nevertheless, the fluctuation of the mean field dose not vanish in the large size limit [2]. Thus, the system has a nontrivial collective motion [5].

From a realistic viewpoint, however, the synchronous updating is not always plausible as models of real systems

*Electronic address: morita@sys.eng.shizuoka.ac.jp

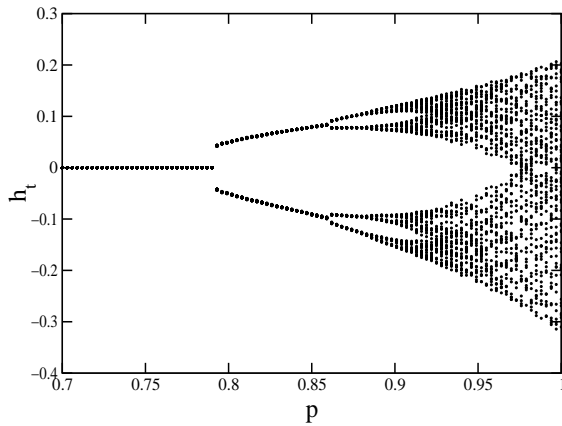


FIG. 1: Bifurcation diagram for evolution of the mean field as function of the updating rate p in the case of $a = 0.9$, $K = 0.7$, $N = 10^5$. For given values of p , the value of the mean field is plotted for 64 successive steps after 10^4 steps as transient.

[17, 18, 19, 20, 21]. In some cases, for example, neural networks, an independent choice of the times at which the state of a given element is updated should provide a better approximation. Abramson and Zanette have numerically found that, for globally coupled logistic map with completely stochastic updating, the fluctuation of the mean field can vanish in the large size limit [19]. In this paper, we study the stochastic updating model as follows

$$x_{t+1}(i) = \begin{cases} f(x_t(i)) + Kh_t & \text{with probability } p \\ x_t(i) & \text{with probability } (1-p) \end{cases} \quad (8)$$

At each time step, update the elements with probability p satisfying $0 < p \leq 1$. When the updating rate p is equal to 1, the model (8) becomes the synchronous updating model (1). On the other hand, when p decreases to 0, the model (8) approaches the completely asynchronous updating model.[24] Thus, the value of $(1-p)$ represents the strength of the asynchronism. The purpose of this paper is to investigate how the collective behavior changes when the updating probability p varies, mainly by the linear stability analysis of the stationary state in the large size limit.

II. NUMERICAL RESULTS

In this section, we present the numerical results for the model (8). First, we examine the case of $a < 1$. When $p = 1$, the synchronized chaos is observed. On the other hand, when $p < 1$, some elements are updated and the others are fixed at each time step. Hence, even when a pair of elements have the same value at a moment, they can have different values at the next time. As a result, the synchronized chaos is broken. When p is near 1, the synchronized state is blurred slightly. As p decreases, a sequence of bifurcations are seen (in Fig. 1). It resembles

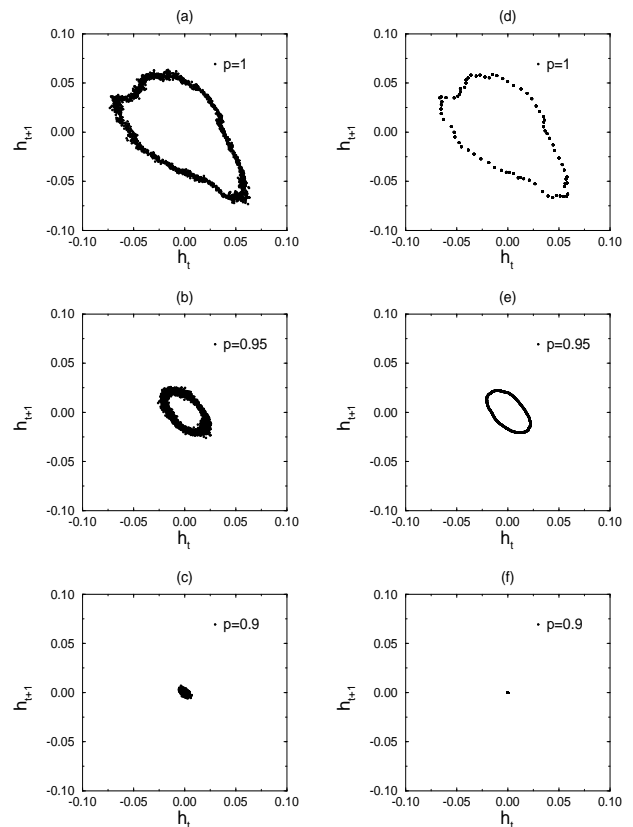


FIG. 2: Examples of the return maps of the mean field are shown ($a = 1.625$, $K = 0.4$). While (a), (b), and (c) are obtained by the direct numerical calculation of (8) with the size of $N = 10^5$, (d), (e), and (f) are obtained by the numerical calculation of (11) with 2^{18} grids. (a) and (d) are for $p = 1$, (b) and (e) are for $p = 0.95$, (c) and (f) are for $p = 0.9$. We plot 2000 points after 10^4 steps as transient.

the period doubling cascade. However, there is a finite jump at this bifurcation in contrast of the usual period doubling bifurcation. This discontinuity is due to the fact that the map $f(x)$ is piecewise linear. When p is smaller than a threshold value p_c , all elements fall into the fixed point (6) and the mean field h_t becomes 0. Thus, the collective motion vanishes below the threshold p_c .

Second, we examine the case of $a > 1$, where the non-trivial collective motion is seen for $p = 1$. Figs. 2(a), 2(b), and 2(c) show the motions of the mean field for some values of p , with $a = 1.625$, $K = 0.4$, and $N = 10^5$. The amplitude of motion of the mean field decreases as p decreases.

It should be noted that the dynamics of each element is not deterministic due to the updating rule. Thus, the mean field value is blurred if the system size is finite. Even for $p = 1$, the finite size effect works on the motion of the mean field as an internal noise [5]. For that reason, it is useful to consider the large size limit. In the large size limit, the ensemble of the elements is characterized by its distribution. In the synchronous updating case,

the evolution of the distribution function $\rho_t(x)$ obeys the nonlinear Frobenius-Perron equation

$$\begin{aligned} \rho_{t+1}(x) &= \mathcal{F}[\rho_t(x); h_t] \\ &\equiv \frac{\rho_t(y_+) + \rho_t(y_-)}{a}, \end{aligned} \quad (9)$$

where \mathcal{F} represents the Frobenius-Perron operator, and y_+ and y_- are the two preimage of x , i.e., $x = f(y_{\pm}) + Kh_t$. Here the mean field is determined in the integral form:

$$h_t = \int g(x)\rho_t(x)dx. \quad (10)$$

In the stochastic updating case ($p < 1$), the evolution of $\rho_t(x)$ is described as

$$\rho_{t+1}(x) = p \mathcal{F}[\rho_t(x); h_t] + (1-p) \rho_t(x). \quad (11)$$

Despite the stochastic updating, the distribution function evolves in the deterministic way.

In order to calculate (11) numerically, we approximate the distribution function $\rho_t(x)$ by dividing the relevant interval of x into m small intervals. The evolution of the distribution is described by the $m \times m$ transfer matrix which depends on time through the mean field h_t . Here we construct the transfer matrix by applying the method by Binder and Campos [22]. Figs. 2(d), 2(e), and 2(f) show the the motion of the mean field calculated by this method with the parameter values corresponding to Figs. 2(a), 2(b), and 2(c), respectively. The direct calculations of (8) compare successfully with the results of (11), except for the fluctuation due to the finite size effect. As is seen from Fig. 2(f), when p is small, the collective motion vanishes like the case of $a < 1$. It should be noted that, in the stationary state, all elements are still scattered and behave chaotically in contrast to the case of $a < 1$. The fluctuation of the mean field resides for finite size systems (Fig. 2(c)).

III. LINEAR STABILITY ANALYSIS OF THE STATIONARY STATES

The result of numerical simulation indicates that there exists a threshold value for updating rate p_c . It is observed that the collective motion vanishes, and the stationary state (with distribution $\rho_t(x) = \rho_*(x)$) is realized for p smaller than p_c . In this section, we present the linear stability analysis of the stationary state to estimate the value of p_c .

First, we consider the case of $a < 1$. This case is simpler, because all elements have the identical fixed value $x_*(> 0)$ in the stationary state. Considering a small perturbation from x_* , we assume that every element has a positive value. Since $\rho_t(x)$ for $x < 0$ is 0, the evolution of $\rho_t(x)$ is rewritten as

$$\rho_{t+1}(x) = \frac{p}{a} \rho_t \left(\frac{a - 2x + 2Kh_t}{2a} \right) + (1-p) \rho_t(x). \quad (12)$$

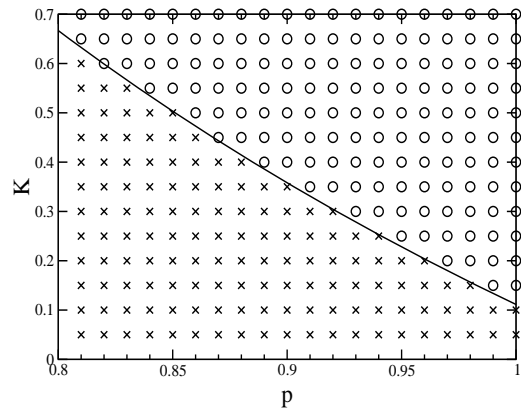


FIG. 3: Phase diagram of the collective motion for $a = 0.9$. The numerical results are obtained for $N = 10^4$. Circles and crosses represent the cases of $\langle h^2 \rangle^{1/2} > 10^{-6}$ and $\langle h^2 \rangle^{1/2} < 10^{-6}$, respectively. Here the angle bracket denotes the average value of the enclosed quantity over 2000 time steps. The solid line represents the theoretical prediction (14).

From (10) and (12), we obtain the dynamics of the mean field obeys

$$h_{t+1} = (-ap - apK + 1 - p) h_t. \quad (13)$$

Thus, the stationary state is stable when $|-ap - apK + 1 - p| < 1$. Consequently, the threshold value p_c is estimated as

$$p_c = \frac{2}{a(1+K) + 1}. \quad (14)$$

In the case of Fig. 2, $p_c = 0.790 \dots$. The theoretical prediction agrees well with the numerical simulation (see also Fig. 3).

Second, we consider the case of $a > 1$. The stationary distribution function $\rho_*(x)$ is expanded into series of step functions as follows [9, 12]

$$\begin{aligned} \rho_*(x) &= \sum_{k=1} C_k \theta(x - X_k) \\ X_k &\equiv f^k(0) \\ C_k &\equiv C_1 \{(f^{k-1})'(f(0))\}^{-1}, \end{aligned} \quad (15)$$

where $\theta(x)$ is a step function: 1 for $x \geq 0$ and 0 for $x < 0$. Thus, X_k and C_k represent the locations and the heights of the steps in $\rho_*(x)$, respectively. We choose C_1 to satisfy the normalization condition

$$-\sum_{k=1} C_k X_k = \int dx \rho_*(x) = 1. \quad (16)$$

If there exists such k_p that satisfies $f^{k_p}(0) = 0$ and $f^k(0) \neq 0$ for $\forall k < k_p$, the sum over k is taken from 1 to k_p . Otherwise, the sum is taken from 1 to ∞ .

Before treating the case of stochastic updating, let us analyze how the stationary state is affected by adding external force with infinitesimal amplitude δ for $p = 1$

and $K = 0$. Here we assume that the external force changes x_i for every element by the given amount. Thus, when the force δ_0 is applied at $t = 0$, the distribution function at $t = 1$ is expressed as

$$\rho_1(x; \delta_0) = \rho_*(x - \delta_0). \quad (17)$$

In the limit of $\delta_0 \rightarrow 0$, the response of the mean field after τ steps is written as

$$h_\tau = L_\tau \delta_0 \quad (18)$$

where L_τ is the linear coefficient for the response with delay of τ steps [12]. From (15), we calculate L_τ as follows

$$L_\tau = - \sum_{k=1}^{\infty} C_k X_{k+\tau}. \quad (19)$$

When the temporal series of the external force is given as $\{\delta_t\}$, the mean field h_t is obtained as

$$h_t = \sum_{\tau=1}^{\infty} L_\tau \delta_{t-\tau}, \quad (20)$$

within the linear approximation. Introducing a cut-off d , the state at the time t can be described approximately by d -dimensional vector

$$\mathbf{v}_t \equiv (\delta_{t-1}, \delta_{t-2}, \delta_{t-3}, \dots, \delta_{t-d}). \quad (21)$$

In order to obtain the stability condition accurately, we must take the limit of $d \rightarrow \infty$. When the components of \mathbf{v}_t is denoted as v_t^i , we obtain

$$h_t = \sum_{i=1}^d L_i v_t^i. \quad (22)$$

The next step is to consider the case of $p = 1$ and $K \neq 0$. In this case, the mean field coupling yields the feedback force. The influence of the feedback force is described as

$$v_{t+1}^1 = K h_t. \quad (23)$$

Taking (22) into account, the evolution of v_t^i is described as

$$v_{t+1}^i = \sum_{j=1}^d J_{ij} v_t^j, \quad (24)$$

where the matrix J_{ij} is given by

$$J_{ij} = \begin{pmatrix} KL_1 & KL_2 & KL_3 & \cdots & KL_{\tau_c-1} & KL_{\tau_c} \\ 1 & 0 & 0 & \cdots & 0 & 0 \\ 0 & 1 & 0 & \cdots & 0 & 0 \\ \vdots & \vdots & \vdots & \ddots & \vdots & \vdots \\ 0 & 0 & 0 & \cdots & 0 & 0 \\ 0 & 0 & 0 & \cdots & 1 & 0 \end{pmatrix}. \quad (25)$$

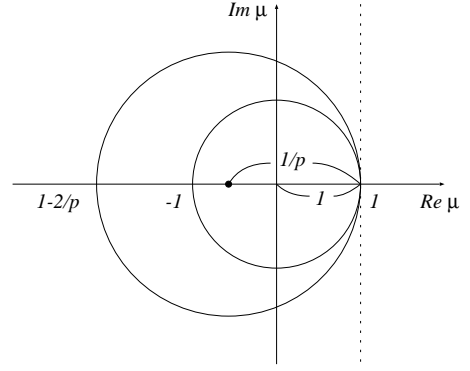


FIG. 4: The stability condition. If all solutions μ_i of (26) lie within the large (unit) circle, the stationary state is stable for $p < 1$ ($p = 1$). Thus, all μ_i lie on the left of the dotted line, there exists threshold value p_c .

The characteristic equation of the matrix (25) is given as

$$\lambda^d = K \sum_{i=1}^d L_i \lambda^{d-i}, \quad (26)$$

which coincides with the results of Refs. [12, 23]. The roots of (26) are denoted as μ_i . In the case of the synchronous updating ($p = 1$), if all μ_i lie within the unit circle in the complex plane, the stationary state is stable [23].

Let us now return to the asynchronous updating case ($p < 1$). Here we define the vector \mathbf{v}_t to satisfy (22). Thus, v_t^i represents the contribution from the past perturbations through i times of updating. Taking into account that the elements are updated with probability p and fixed with probability $1 - p$, we obtain

$$v_{t+1}^i = \sum_{j=1}^d [p J_{ij} + (1 - p) \delta_{ij}] v_t^j. \quad (27)$$

The characteristic equation for (27) is given as

$$\left(\frac{\lambda - 1 + p}{p} \right)^d = K \sum_{i=1}^d L_i \left(\frac{\lambda - 1 + p}{p} \right)^{d-i}. \quad (28)$$

Comparing (28) with (26), λ in (26) is replaced with $(\lambda - 1 + p)/p$ in (28), and thus the stability condition for (27) becomes

$$|1 - p + p \mu_i| < 1 \quad (\text{for all } i). \quad (29)$$

This condition means all μ_i lie within the circle with center $(1 - 1/p, 0)$ and radius $1/p$ in the complex plane (Fig. 4). In the limit $p \rightarrow 0$, the condition (29) becomes $Re(\mu_i) < 1$. Consequently, if all μ_i satisfy $Re(\mu_i) < 1$, the system has the threshold p_c .

For example, we investigate a simple case $a = (1 + \sqrt{5})/2$, where $f^3(0) = 0$. Thus, k_p is 3 and X_k is periodic. In this case, the characteristic equation (26) can be solved

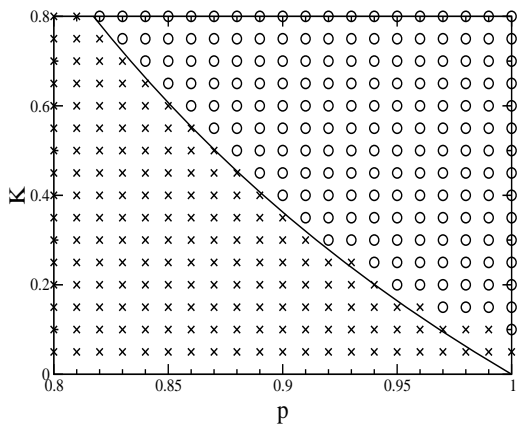


FIG. 5: Phase diagram of the collective motion for $a = (1 + \sqrt{5})/2$. The numerical results are obtained by calculation of (11) with 2^{18} grids. Circles and crosses represent the cases of $\langle h^2 \rangle^{1/2} > 10^{-12}$ and $\langle h^2 \rangle^{1/2} < 10^{-12}$, respectively. The solid line represents the theoretical prediction (33).

analytically in the limit of $d \rightarrow \infty$. From (15) and (19), the linear coefficient $\{L_t\}$ is given as

$$\begin{aligned} L_{3n+1} &= L_1 = -\frac{5 + \sqrt{5}}{10}, \\ L_{3n+2} &= L_2 = -\frac{5 - \sqrt{5}}{10}, \\ L_{3n+3} &= L_3 = 1. \end{aligned} \quad (30)$$

Let us assume that μ satisfies condition $|\mu| > 1$. Then we rewrite the characteristic equation (26) in the limit $d \rightarrow \infty$ as follows:

$$\begin{aligned} 1 &= K \sum_{i=1}^{\infty} L_i \mu^{-i} \\ &= K \frac{L_1 \mu^{-1} + L_2 \mu^{-2} + L_3 \mu^{-3}}{1 - \mu^{-3}}. \end{aligned} \quad (31)$$

From this, μ is given as

$$\mu = \frac{KL_1 - 1 \pm \sqrt{(KL_1 - 1)^2 - 4K - 4}}{2}. \quad (32)$$

When $(45 - 21\sqrt{5})/2 < K < (5 + 3\sqrt{5})/2$, the part in the square root in (32) is negative and thus the solution (32) is complex conjugate pair. Then, we obtain $|\mu| = \sqrt{K+1}$. Thus, $|\mu| > 1$ holds for $0 < K < (5 + 3\sqrt{5})/2$. In this case, the threshold p_c is given by

$$p_c = \frac{KL_1 - 3}{KL_1 - 3 - K} \quad (33)$$

Figure 5 shows the correspondence between the above estimation for p_c and the numerical results. It indicates the good agreement, except for the lower right corner. The estimation implies p_c tends to 1 in the limit of $K \rightarrow 0$, and we think that the gap in the corner appeared because the amplitude of the collective motion for small K is very small (estimated at $\exp(-C/K)$ for the case with $p = 1$ [11, 12]).

For such special values of a , where $\{X_k\}$ falls on a periodic orbit, we can solve the characteristic equation by the above method. In this case, the characteristic equation has no solution μ which satisfies $\text{Re}(\mu) > 1$ for adequately weak coupling. Thus there exists the threshold. For the general values of a , however, it is difficult to solve the characteristic equation and we have not obtained the stability condition explicitly at present.

IV. SUMMARY AND REMARKS

This study have explored the globally coupled tent maps with stochastic updating. We introduced the updating rate p and examined how the collective behavior changes as p varies. In the case of $a < 1$, the collective motion has a sequence of bifurcations, which is similar to the period doubling cascade. In the case of $a > 1$, the amplitude of the collective motion decreases as p decreases. For the both cases, we observed the threshold p_c , below which the collective motion vanishes. We estimated successfully the threshold p_c by the linear stability analysis of the stationary state.

For weak coupling, the threshold p_c is likely to remain near 1 as is seen for the example $a = (1 + \sqrt{5})/2$. Thus, a tiny asynchronism may extinguish the collective motion. Therefore, when GCM is used as model of real systems, we keep in mind that even if the updating rule is almost synchronous, the effect of asynchronous updating should not be ignored.

Acknowledgements

This research was supported partly by Japan Society of Promotion of Science under the contract number RFTF96I00102.

[1] K. Kaneko, *Physica* **41D**, 137 (1990).
 [2] K. Kaneko, *Phys. Rev. Lett.* **65**, 1391 (1990); *Physica* **55D**, 368 (1992).

[3] H. Chaté and P. Manneville, *Europhy.Lett.* **17**, (1991) 409; **17**, (1992) 291; *Prog. Theor. Phys.* **87**, 1 (1992).
 [4] N. Nakagawa and Y. Kuramoto, *Prog. Theor. Phys.* **89**,

- 313 (1993).
- [5] A.S. Pikovsky and J. Kurths, Phys. Rev. Lett. **72**, 1644 (1994); Physica **76D**, 411 (1994).
- [6] K. Kaneko, Physica **86D**, 158 (1995).
- [7] W. Just, J. Stat. Phys. **79**, 429 (1995); Physica **81D**, 317 (1995)
- [8] S.V. Ershov and A.B. Potapov, Physica **86D**, 532 (1995); **106D**, 9 (1997).
- [9] S. Morita, Phys. Lett. A **211**, 258 (1996).
- [10] S. Morita, Phys. Lett. A **226**, 172 (1997).
- [11] N. Nakagawa and T.S. Komatsu, Phys. Rev. E **57**, 1570 (1998); **59**, 1675 (1998).
- [12] T. Chawanya and S. Morita, Physica **116D**, 44 (1998).
- [13] T. Shibata, T. Chawanya, and K. Kaneko, Phys. Rev. Lett. **82**, 4424 (1999).
- [14] T. Shibata and K. Kaneko, Physica **124D**, 177 (1998).
- [15] G. Pérez and H.A. Cerdeira, Phys. Rev. Lett. **46**, 7492 (1992).
- [16] G. Pérez, S. Sinha, and H.A. Cerdeira, Physica **63D**, 341 (1993).
- [17] G. Pérez, S. Sinha, and H.A. Cerdeira, Phys. Rev. E **54**, 6936 (1996).
- [18] J. Rolf, T. Bohr, and M.H. Jensen, Phys. Rev. E **57**, R2503 (1998).
- [19] G. Abramson and D.H. Zanette, Phys. Rev. E **58**, 4454 (1998).
- [20] S. Sinha, Phys. Rev. E **57**, 4041 (1998).
- [21] H.J. Blok and B. Bergersen, Phys. Rev. E **59**, 3876 (1999).
- [22] P.-M. Binder and D.H. Campos, Phys. Rev. E **53**, R4259 (1996).
- [23] G. Keller, Prog. Prob. **46**, 183 (2000).
- [24] For $p = 0$, all elements are never updated. Therefore, when we consider the limit of $p \rightarrow +0$, the time t must be rescaled by p to keep the motions.